Magnesium Technology 2012
Edited by: Suveen N. Mathaudhu, Wim H. Sillekens, Neale R. Neelameggham, and Norbert Hort
TMS (The Minerals, Metals & Materials Society), 2012

STRUCTURAL ORIGIN OF REVERSIBLE TWINNING, NON-SCHMID EFFECT, INCOHERENT TWIN BOUNDARIES AND TEXTURE IN HEXAGONAL CLOSE-PACKED METALS

B. Li [1,2], H. El Kadiri [1,3], X.Y. Zhang [4], S.N. Mathaudhu [5], Q. Ma [1]
[1] Center for Advanced Vehicular Systems, Mississippi State University, Starkville, MS 39759, USA
[2] Center for Advanced Metallic and Ceramic Systems, Johns Hopkins University, Baltimore, MD 21218, USA
[3] Department of Mechanical Engineering, Mississippi State University, Starkville, MS 39759, USA
[4] School of Materials Science and Engineering, Chongqing University, Chongqing, China
[5] Weapons and Materials Research Directorate, U.S. Army Research Laboratory, Aberdeen Proving Ground, MD
Keywords: Keyword1, Keyword2, Keyword3, etc.

Abstract

Notably the most dominant twinning mode in hexagonal close-packed metals, $\{10\bar{1}2\}<10\bar{1}\bar{1}>$ twinning presents abnormal properties such as reversible twinning and non-Schmid effect. The twin boundaries may significantly deviate from the $\{10\bar{1}2\}$ twinning plane. HCP metals also present a strong propensity to develop texture during processing. Through electron backscatter diffraction and high resolution transmission electron microscopy observations, we show that these properties can be well understood from the perspective of the atomic shuffling that dominates in the twinning.

Introduction

Due to the insufficient number of easy slip systems in low symmetry hexagonal close-packed (HCP) metals, e.g., magnesium (Mg), titanium (Ti), zirconium (Zr) and cobalt (Co), profuse twinning is activated during plastic deformation to accommodate the strain perpendicular to the basal plane, i.e., along the direction of <*c*>-[0001]. The ubiquitous $\{10\bar{1}2\}<10\bar{1}\bar{1}>$ twinning is the most commonly observed and dominant twinning mode in HCP metals. The properties of this particular twinning mode are distinctive in comparison to those of other twinning modes:

(1) *Reversible twinning.* Detwinning [1,2] can occur if the applied external load is removed or reversed. Twin boundaries (TBs) may move backward and shrink the twins, giving rise to the pseudoelasticity [3] in HCP metals;
(2) *Non-Schmid effect.* The Schmid Law can be violated. Barnett et al. [4] found that, in the $\{10\bar{1}2\}+\{10\bar{1}1\}$ double twinning, the secondary $\{10\bar{1}2\}$ twinning does not follow the Schmid Law;
(3) *Extremely incoherent TBs.* Partridge and Roberts [5] observed abnormal TB migration in Mg by optical microscopy. They found that, under small stresses from indentation, the existing $\{10\bar{1}2\}$ TBs can migrate and evolve into extremely incoherent structures which considerably deviate from the $\{10\bar{1}2\}$ twinning plane. In other words, the TBs no longer coincide with the $\{10\bar{1}2\}$ twinning plane.

Additionally, Mg and other HCP metals have a strong propensity for developing pronounced texture during mechanical processing. During rolling or extrusion, the basal planes of the crystallites are reoriented roughly parallel to the rolling or extrusion direction [6,7]. Basal texture has also been reported after grain refining by severe plastic deformation (SPD) [8]. Karaman et al. [9] studied the texture of Zr, beryllium (Be), AZ31 Mg alloy and Ti-6Al-4V alloy after each was subjected to one pass of equal channel angular extrusion (ECAE). They found that the basal planes always aligned with the most elongated direction of the sheared grains, irrespective of the *c/a* ratio, grain size and initial texture. Their visco-plasticity-self-consistent (VPSC) modeling showed that basal slip must be the primary slip system in all four materials, contributing to the texture, when twinning was not considered in the modeling. In fact, the $\{10\bar{1}2\}<10\bar{1}\bar{1}>$ twinning is a major contributor to texture in HCP metals [10] because twinning reorients the parent lattice much more efficiently than dislocation slip.

A question immediately arises: intrinsically, how are these aforementioned properties of HCP metals originated from the perspective of crystal structure? The purpose of this work is to address this important question based upon our experimental observations.

Experimental Methods

An AM30 Mg alloy (composition) was pre-extruded and then compressed along the extrusion direction (ED) until 2.3% plastic strain. The microstructures of the pre-extruded and the deformed samples were examined with field emission gun scanning electron microscopy (FEG-SEM) equipped with an electron back-scatter diffraction (EBSD) data acquisition and analysis system. The sample was polished at a section normal to radial direction of the extruded billet. Pure, polycrystalline Co samples were also deformed dynamically at room temperature [11], and the microstructure of the tested samples was examined by transmission electron microscopy (TEM) and high resolution TEM (HRTEM).

Results

Figure 1(a) shows the inverse pole figure mapping the misorientations in the deformed AM30 sample. The elongated grains (in blue) experienced large plastic strain during extrusion, and the elongation paralleled the extrusion direction (ED). The variation in the blue background indicates a relatively high density of dislocations and substructures in these grains. In contrast, the fine, equiaxed grains (in green) are dynamically recrystallized during extrusion with a low density of dislocations. Compression along the ED activated the $\{10\bar{1}2\}<10\bar{1}\bar{1}>$ twinning. The needles (in red) are deformation twins that cross the elongated grains. With orientation analysis, the traces of the

twinning planes (must be one of the $\{10\bar{1}2\}$ planes) can be determined. Figure 1(b) shows a magnified view that highlights the twins. Three intercrossing white lines mark the traces of the $\{10\bar{1}2\}$ planes in the parent lattices. There should be six $\{10\bar{1}2\}$ planes and hence six such traces. Since three of the traces almost coincide with the others, three lines suffice to demonstrate the deviation. Strikingly, the TBs do not coincide with the traces of the $\{10\bar{1}2\}$ plane. Additional scanning in different regions and grains shows similar results, with most TBs deviating from the $\{10\bar{1}2\}$ twinning plane.

Large deviation was also revealed in deformation twins in Co samples. Figure 2 shows a HRTEM micrograph of the $\{10\bar{1}2\}<10\bar{1}\bar{1}>$ TBs and the traces of the twinning planes. Lattice fringes from the basal planes can be seen. In the inset of Figure 2, the diffraction pattern indicates the grains indeed satisfy the $\{10\bar{1}2\}<10\bar{1}\bar{1}>$ twin relationship. The zone axis is parallel to $[\bar{1}2\bar{1}0]$ direction. The TBs, twinning planes, and the basal planes of the twin and the parent are all parallel to the zone axis. In this orientation, there are only two possible twinning planes, and their traces are marked with two broken lines. It can be seen that the actual TBs deviate strikingly far from the $\{10\bar{1}2\}$ twinning plane. In fact, the TB near the top is almost parallel to the basal plane of the parent.

Analysis and Discussion

The large deviation between the actual TBs and the $\{10\bar{1}2\}$ twinning plane observed in our EBSD and HRTEM examinations indicates that the $\{10\bar{1}2\}<10\bar{1}\bar{1}>$ twinning mode may be mechanistically different from other twinning modes in which twinning dislocations control twin growth [12]. Along with the reversible twinning and the non-Schmid effect, these abnormal properties call into a question whether this twinning mode is truly controlled by twinning dislocations.

The crystallographically-defined Burgers vector of the elementary twinning dislocation [13] on the $\{10\bar{1}2\}$ plane equals

$$b_T = \frac{(3-\gamma^2)\cdot a}{2\sqrt{3+\gamma^2}}, \quad (1)$$

where a is the lattice parameter (0.321 nm for Mg) and γ the c/a ratio (1.624 for Mg). We can calculate the magnitude of the Burgers vector for Mg as 0.024 nm, which is less than one tenth of the Burgers vector of the basal dislocations. That the twinning dislocation has such a tiny Burgers vector significantly implies that the twin lattice exists almost in the parent lattice before any twinning shear is applied. In other words, negligible shear is needed and only local atomic shuffling is required to accomplish the twinning.

Figure 3 schematically demonstrates how the $\{10\bar{1}2\}<10\bar{1}\bar{1}>$ twinning is achieved by atomic shuffling rather than twinning dislocation. In fact, the $\{10\bar{1}2\}$ twin can be constructed directly from the parent without involving any well-defined twinning dislocations at the TB. Details of this concept can be found elsewhere [14]. Here we provide a brief description of the theory. In Figure 3, the parent HCP lattice is plotted to show the *...ABABABAB...* stacking sequence of the basal planes perpendicular to the paper plane. If we connect those atoms with distances ~ a (the lattice parameter), immediately we can see that a new hexagonal lattice can be constructed with the new basal planes at a misorientation of 90° with respect to the basal plane of the parent lattice. The two lattices indeed satisfy the $\{10\bar{1}2\}<10\bar{1}\bar{1}>$ twin relationship because the $\{10\bar{1}2\}$ plane (the shaded plane in Figure 3) is common to both lattices. The basal planes of the twin are marked by A' and B', parallel to the figure plane. The basal planes of the parent and the twin are perpendicular to each other, obviously satisfying the twin orientation relationship. However, the twin lattice does not have the correct HCP packing, as can be seen both from the constructed prism plane that is flat but should be double-layered, as well as from the constructed basal plane which is double-layered but should be flat. To correct these distortions and packing "errors", atomic shuffling is required: the pink atoms on the new basal (A') plane have to shuffle outward to make the new basal plane flat, while the atoms of the B' plane have to shuffle downward to make the new prism plane double-layered. These shuffles, together with others, are concerted to reach the correct c/a ratio with magnitudes much smaller than any known dislocation Burgers vectors in the parent lattice; likewise, the shuffles convert the parent basal planes into the twin prism planes and the parent prism planes into the twin basal planes.

It should be noted that the atomic shuffling-dominated twinning mechanism for the $\{10\bar{1}2\}<10\bar{1}\bar{1}>$ mode is *not* at odds with the classical twinning theory [15] in which a homogeneous shear and atomic shuffling must generally be involved at the same time for twinning in HCP metals. As pointed out by Christian and Mahajan [16], for HCP metals, atomic shuffling may be as important as the magnitude of shear in controlling the operative twinning modes. According to our simulations and calculations, the amount of the shear (i.e., the Burgers vector of the elementary twinning dislocation) and the magnitude of the shuffle of each twinning mode, i.e., $\{10\bar{1}\bar{1}\}<10\bar{1}\bar{2}>$, $\{10\bar{1}2\}<10\bar{1}\bar{1}>$, $\{11\bar{2}1\}<11\bar{2}\bar{6}>$ and $\{11\bar{2}2\}<11\bar{2}\bar{3}>$, drastically vary from one twinning mode to another. The $\{10\bar{1}2\}<10\bar{1}\bar{1}>$ mode is an extreme case in which shear is negligible and shuffle is dominant (as shown in Figure 3); the $\{11\bar{2}1\}<11\bar{2}\bar{6}>$ mode is an extreme case in which shear is dominant and no shuffle is involved; the $\{10\bar{1}\bar{1}\}<10\bar{1}\bar{2}>$ mode is shear dominant with minor off-plane shuffles, i.e., the atoms have to shuffle slightly off the $\{10\bar{1}\bar{1}\}$ twinning plane [12]; and the $\{11\bar{2}2\}<11\bar{2}\bar{3}>$ mode is middle-ground where shear and shuffle are nearly equal, and the shuffles are confined in-plane [17]. From this point of view, our shuffling model (Figure 3) is an extreme case that still falls inside the classical framework of twinning theory. Nonetheless, there is no unified dislocation model that is able to describe all these major twinning modes in HCP metals and also account for the diversity of shear and shuffle of the individual twinning modes.

The $\{10\bar{1}2\}<10\bar{1}\bar{1}>$ twinning reorients the *c*-axis of the parent lattice by about 90° around the $<\bar{1}2\bar{1}0>$ direction, which is the normal of the plane of shear. If we detach the two lattices in Figure 3, as shown in Figure 4, it is clear that there is a misfit in lengths between the two lattices in the direction of the *c*-axis of the parent lattice. Hence, a misfit strain is created by the $\{10\bar{1}2\}<10\bar{1}\bar{1}>$ twinning. This misfit strain (ε) along the *c*-axis of the parent equals

$$\varepsilon = \frac{\sqrt{3}-\gamma}{\gamma}. \quad (2)$$

The value of the misfit strain varies as a function of γ (ε = 9.1% for Ti, and 6.7% for Mg). Accordingly, for those HCP metals with a *c/a* ratio less than $\sqrt{3}$ (e.g., Mg, Ti, Zr, Co, Be etc.), a positive tensile stain is produced; for those HCP metals with a *c/a* ratio greater than $\sqrt{3}$ (e.g., Cd and Zn), a negative compressive strain is produced. Therefore, for Mg alloys, the $\{10\bar{1}2\}<10\bar{1}\bar{1}>$ twinning efficiently accommodates the elongation if a tensile load is applied parallel to the *c*-axis of the parent, but the shear strain is negligible because this twinning mode is dominated by atomic shuffling. This analysis is essentially the same as Yoo's pioneering work [18] in which the well-known "$\sqrt{3}$ criterion" was established but in a more explicit fashion.

The atomic shuffling-dominated $\{10\bar{1}2\}$ twinning entails very low critical stress for twin growth, which is confirmed by early experimental observations. Partridge and Roberts [5] studied the movement of the $\{10\bar{1}2\}<10\bar{1}\bar{1}>$ twinning in Mg under small stresses with micro-hardness indenter. Figure 4 immediately reveals that, under an external load, intrinsically HCP metals have a tendency to reorient the basal planes to the direction parallel to the maximum elongation direction of deformed grains, as observed by Karaman et al [9]. As a result, in extrusion and rolling processes, the basal planes will be reoriented parallel to the extrusion or the rolling direction.

Generally, small deviations between the twinning plane and the TB are allowed when twin accommodation is required [5], but such deviations do not exceed a few degrees. Small deviations may also be allowed by the presence of twinning dislocation loops at a TB. The abnormal TB migration observed by Partridge and Roberts [5], and the large deviation between the actual TB and the $\{10\bar{1}2\}$ twinning plane observed in this work, can both be well understood with the shuffling mechanism: because the migration of the TB is dominated by atomic shuffling instead of shear, the actual TB does not have to match the crystallographic twinning plane.

Finally, the structural origin of the reversible $\{10\bar{1}2\}<10\bar{1}\bar{1}>$ twinning is well explained, as can be readily seen from Figure 3, by shuffling-dominated twinning. The conversions between the parent lattice and the twin lattice are reversible. Upon unloading or removal of the load, the atoms at TBs may shuffle back and move the TBs backward. The driving force is the local strain and the twin/parent interfacial energy.

Conclusions

Using EBSD and TEM, we measured the traces of $\{10\bar{1}2\}$ twin boundaries in Mg and Co and revealed a large deviation between the twinning plane and the twin boundaries. These results confirm that $\{10\bar{1}2\}$ twinning is dominated by atomic shuffling. This conclusion well explains the structural origin of reversible twinning, non-Schmid effect and texture in HCP metals.

Acknowledgements

This work was partly supported at Center for Advanced Metallic and Ceramic Systems, Johns Hopkins University, by ARMAC-RTP, DAAD19-01-2-0003 and W911NF-06-2-0006. B. Li, H. El Kadiri, and Q. Ma gratefully acknowledge support from the Center for Advanced Vehicular Systems, Mississippi State University. Thanks are extended to H.R. Wainwright for her assistance with the preparation of the manuscript.

References

[1] L. Wu, A. Jain, D. W. Brown, g. M. Stoica, S. R. Agnew, B. Clausen, D.E. Fielden, P.K. Liaw, "Twinning–detwinning behavior during the strain-controlled low-cycle fatigue testing of a wrought magnesium alloy ZK60", Acta Mater 56, (2008) 688-695.

[2] A. Jain, S. R. Agnew, "Modeling the temperature dependent effect of twinning on the behavior of magnesium alloy AZ31B sheet", Mater Sci Eng A 462(2007)29-36.

[3] C.H. Caceres, T. Sumitomo, M. Veidt, "Pseudoelastic behaviour of cast magnesium AZ91 alloy under cyclic loading–unloading", Acta Mater 51 (2003) 6211-6218.

[4] M.R. Barnett, Z. Keshavarz, A.G. Beer, X. Ma, "Non-Schmid behaviour during secondary twinning in a polycrystalline magnesium alloy", Acta Mater 56 (2008) 5-15.

[5] P.G. Partridge, E. Roberts, "The formation and behaviour of incoherent twin boundaries in hexagonal metals", Acta Met 12 (1964) 1105-1210.

[6] J. Bohlen, M. R. Nurnberg, J. W. Senn, D. Letzig, S. R. Agnew, "The texture and anisotropy of magnesium–zinc–rare earth alloy sheets", Acta Mater 55(2007)2101-2112.

[7] S. R. Angew, J. A. Horton, T. M. Lillo, D. W. Brown, "Enhanced ductility in strongly textured magnesium produced by equal channel angular processing", Scripta Mater 50(2004)377-381.

[8] R. Z. Valiev and T. G. Langdon, "Principles of equal-channel angular pressing as a processing tool for grain refinement", Prog. Mater. Sci. 51(2006)881-981.

[9] G. G. Yapici, I. Karaman, "Common trends in texture evolution of ultra-fine-grained hcp materials during equal channel angular extrusion", Mat Sci Eng A, 503 (2009) 78-81.

[10] J. J. Fundenberger, M. J. Phillipe, F. Wagner, C. Esling, "Modelling and prediction of mechanical properties for materials with hexagonal symmetry (zinc, titanium and zirconium alloys)", Acta Mater 45(1997) 4041-4055.

[11] X.Y. Zhang, Y.T. Zhu, Q. Liu, "Deformation twinning in polycrystalline Co during room temperature dynamic plastic deformation", Scripta Mater 63 (2010) 387-390.

[12] B. Li, E. Ma, "Zonal dislocations mediating $\{10\bar{1}1\}<10\bar{1}2>$ twinning in magnesium", Acta Mater 57 (2009) 1734-1743.

[13] N. Thompson, D. J. Millard, "Twin formation in cadmium", Phil Mag 43 (1952) 422.
[14] B. Li, E. Ma, "Atomic shuffling dominated mechanism for deformation twinning in magnesium", Phys Rev Lett, 103 (2009) 035503.
[15] B.A. Bilby, A.G. Crocker, "The theory of the crystallography of deformation twinning", Proc Roy Soc. A, 288 (1965) 240-255.
[16] J.W. Christian, S. Mahajan, "Deformation twinning", Prog. Mater Sci 39 (1995) 1-157.
[17] B. Li, H. El Kadiri, M.F. Horstemeyer, "Extended zonal dislocations mediating $\{1\bar{1}22\} < 1\bar{1}\overline{23} >$ twinning in titanium", Philo Mag 2011, accepted.
[18] M.H. Yoo, "Slip, twinning, and fracture in hexagonal close-packed metals", Met Trans A, 12A, 1981: 409-418.

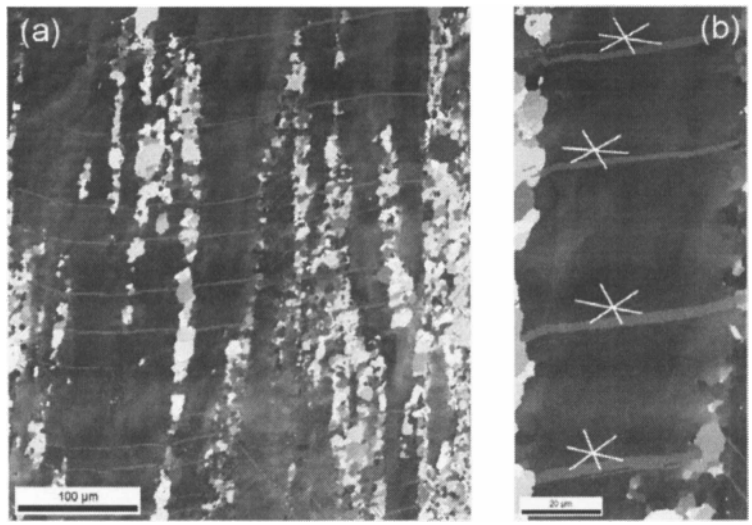

Figure 1. (a) Mapping of misorientations in a pre-extruded AM30 Mg alloy after compression along the extrusion direction (ED, vertical direction). The elongated grains have a relatively high density of dislocations; whereas the fine, equiaxed grains are dynamically recrystallized during extrusion with a low density of dislocations. The needles are deformation twins mostly in the elongated grains. (b) A magnified view of (a) highlights the twins. A group of white lines mark the traces of the $\{10\bar{1}2\}$ planes in the matrix. There are six $\{10\bar{1}2\}$ planes and hence six traces, but three of the traces almost coincide with the others, thus we only plot three markings. As is apparent, the twin boundaries deviate from the traces of the $\{10\bar{1}2\}$ plane.

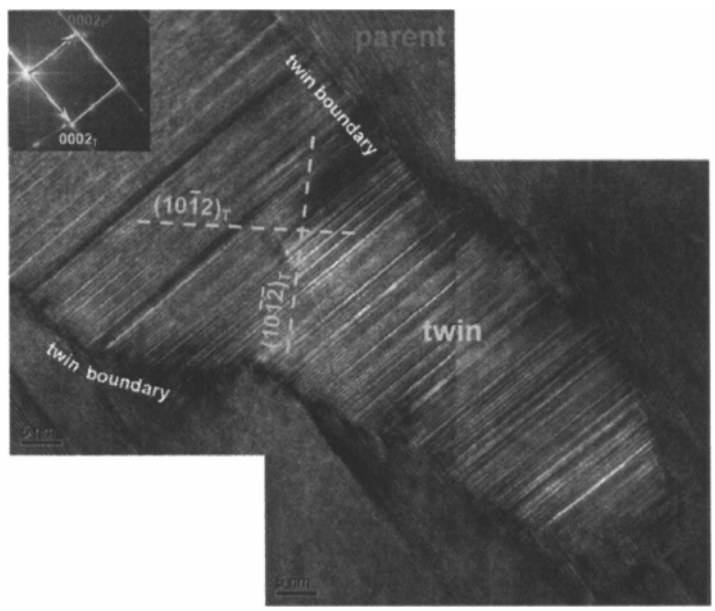

Figure 2. A high Resolution TEM micrograph shows deformation twins in dynamically compressed Co. The diffraction pattern in the inset indicates that the twin and the parent satisfy the $\{10\bar{1}2\}<10\bar{1}\bar{1}>$ twin relationship (zone axis $[\bar{1}2\bar{1}0]$). In this orientation, the two possible $\{10\bar{1}2\}$ twinning planes are marked with broken lines. We can see the actual twin boundaries deviate strikingly far from the twinning planes (> 45°). The deviation can also be appreciated by noticing that the top twin boundary is nearly parallel to the basal plane of the parent.

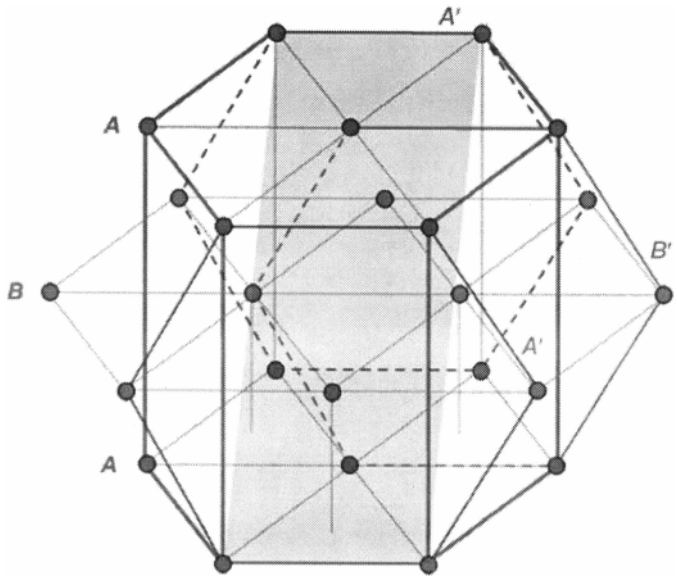

Figure 3. Construction of a new HCP lattice (basal planes are parallel to the paper plane and labeled as *A'B'A'B'*...) from an existing HCP lattice (basal planes are perpendicular to the paper plane and labeled as *ABAB*...). The two lattices share a common $\{10\bar{1}2\}$ plane (the shaded, inclined plane); hence, they satisfy the twin relationship. Local shuffling is required to correct the distortion in the new HCP lattice such that correct stacking sequence and the *c/a* ratio can be established.

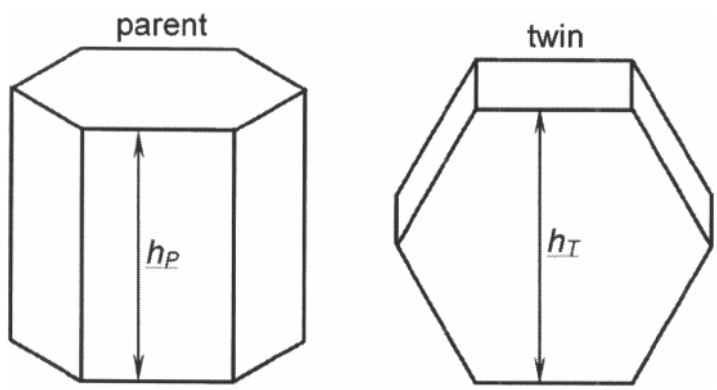

Figure 4. After $\{10\bar{1}2\} < 10\bar{1}\bar{1} >$ twinning, the parent lattice is rotated by 86.3° around $< \bar{1}2\bar{1}0 >$, which produces a misfit strain between the parent and the twin lattices: $\varepsilon = (h_T - h_P)/h_P = (\sqrt{3} - \gamma)/\gamma$ (γ is the *c/a* ratio). For Mg (γ= 1.624), the twinning produces 6.7% tensile strain along the *c*-axis of the parent lattice.